A&A 469, 771–776 (2007)
DOI: 10.1051/0004-6361:20077286

Astronomy & Astrophysics

Photometry and imaging of comet C/2004 Q2 (Machholz) at Lulin and La Silla

Z. Y. Lin[1], M. Weiler[2], H. Rauer[2], and W. H. Ip[1]

[1] Institute of Astronomy, National Central University, 300 Jungda Rd, Jungli City, Taiwan
e-mail: s1249002@cc.ncu.edu.tw
[2] Institut fur Planetenforschung, DLR, Rutherfordstr. 2, 12489 Berlin, Germany

Received 13 February 2007 / Accepted 20 March 2007

ABSTRACT

Aims. We have investigated the development of the dust and gas coma of the comet C/2004 Q2 (Machholz) from December 2004 to January 2005 using observations obtained at the Lulin Observatory, Taiwan and the European Southern Observatory at La Silla, Chile.
Methods. We determined the dust-activity parameter $Af\rho$ and the dust color and derived Haser production rates and scale lengths of C_2 and NH_2. An image enhancement technique was applied to study the morphology of the gas and dust coma.
Results. Two jets were observed in the coma distributions of C_2 and CN of comet Machholz that were not formed in the dust coma. The jets showed a spiral-like structure and pointed at different position angles at different observing times. The formation of these jets can be explained by the presence of two active surface regions on a rotating cometary nucleus.

Key words. comets: indvidual: C/2004Q2 (Machholz)

1. Introduction

Comet C/2004 Q2 (Machholz), moving on an orbit with an eccentricity of 0.9995 and an inclination to the ecliptic plane of 38.6°, was discovered by Don Machholz on August 27, 2004 (IAUC 8394, 2004). The orbital period was approximately determined to be 113 000 years (MPC 54558), thereby making comet Machholz a likely member of the distant Oort cloud population of primordial icy objects. Due to proximity to the Earth (0.35 AU) on January 5th, 2005, comet Machholz showed its maximum magnitude ($3 \sim 4$) at the beginning of January and had become a naked-eye object for several weeks. Its perihelion passage, at a heliocentric distance of 1.21 AU, was on January 25, 2005. Sastri et al. (IAUC 8480, 2005) reported a fan-like structure containing up to three jets on the sunward side of cometary coma during early January 2005. From the evolution of these structures, the rotation period of the nucleus of comet Machholz was determined to be 0.38 ± 0.08 days.

In this paper, we describe narrow-band filter imaging observations of comet Machholz performed between early December 2004 and late January 2005. An overview of the observations is presented in Table 1. The observations used narrow-band filters centered on cometary gas emissions of C_2 and NH_2 and the continuum in two wavelength regions. In four nights of the observing programs at Lulin and LaSilla[1], the sky conditions were photometric and the observations of those nights were used for determining the $Af\rho$ parameter and the gas production rates. The observations and their reduction are described in Sect. 2. In Sect. 3, we analyze the dust continuum and gas emissions, and in Sects. 4 and 5, we study the coma morphology and discuss the implications. In Sect. 6, we summarize our results.

[1] Partly based on obvervations collected at the European Southern Observatory, Chile (ESO program 274.C-5020).

2. Observations and data reduction

Two sets of narrow-band filter images are presented in this paper. The first set was obtained using the 1-m telescope of the Lulin Observatory, Taiwan, from December 1, 2004 to January 25, 2005. This time period included the comet's closest approach to Earth (2005 Jan. 5.61, 0.347 AU) and its perihelion passage (2005 Jan. 25.20, 1.21 AU). The observations were made with the ESA Rosetta comet filters (Bockelee-Morvan et al. 2004) centered on the emissions of $C_2(\Delta\nu = 0)$ and $NH_2(0,7,0)$ and on two wavelength ranges containing solar continuum only ("Blue" continuum at 445 nm, $FWHM = 4$ nm and the "Red" continuum at 687.4 nm, $FWHM = 6$ nm). For the Lulin observations, a PI1300B 1340×1300 CCD camera with an effective pixel scale of $0.515''$ pixel^{-1} (Kinoshita et al. 2005) and an AP8 1024×1024 CCD camera with a pixel scale of $0.62''$ pixel^{-1} (Kinoshita et al. 2002) were used. The second set of observations was acquired with the 3.6 m telescope of ESO (European Southern Observatory) in La Silla, Chile, using the EFOSC2 instrument (1030×1030 pixels, pixel size: $0.314''$, FOV $5.39' \times 5.39'$). The observations employed filters centered on the gas emissions of CN ($\Delta\nu = 0$) and $C_2(\Delta\nu = 0)$ and on two continuum regions (442.2 nm and 683.8 nm). More details on the filter properties can be found in Lara et al. (2004).

The data reduction followed standard procedures. Briefly, the procedure began with bias and dark-current subtraction and flat-field correction of all frames. Then the night sky contribution was subtracted. For the observations obtained at the Lulin observatory in December 2004 the night sky level was determined from those parts of the comet images that do not contain contributions from the cometary coma. For the ESO observations in December 2004 and all observations during January 2005, separate sky background images, taken at a position about 0.5° away from the comet's position in the sky, were used for the sky background determination. This procedure was necessary since the

Table 1. Log of observations performed at the Lulin and La Silla observations.

Date UT	r_h (AU)	Δ (AU)	Solar PA (Degree)	Pixel scale (km/pixel)	Θ (Degree)	Filters	CCD	Note
Dec. 01 2004	1.47	0.614	173.6	229.30	30.4	RF	PI1300B	
Dec. 05 2004	1.43	0.566	180.7	211.41	30.3	RF	PI1300B	⋆
Dec. 09 2004	1.41	0.528	187.6	120.25	30.1	ESO	PI1300B	
Dec. 15 2004	1.36	0.460	204.5	171.82	29.7	RF	PI1300B	⋆
Dec. 29 2004	1.27	0.362	239.5	135.21	31.6	RF	PI1300B	
Dec. 30 2004	1.27	0.358	242.6	133.70	32.1	RF	PI1300B	
Jan. 06 2005	1.24	0.347	257.7	129.61	36.8	RF	PI1300B	⋆
Jan. 24 2005	1.21	0.431	245.2	193.81	49.9	RF	AP8	⋆
Jan. 25 2005	1.21	0.441	244.7	198.31	50.4	RF	AP8	

Note: Δ and r_h are the geocentric and heliocentric distances in AU; Solar PA is the position angle of the projected solar direction, measured from North towards East, and Θ is the phase angle, ie., the Sun-comet-observer angle. Filters "RF" means the Rosetta narrowband filters of C_2, NH_2, Blue cont. and Red cont. Filters "ESO" means images were taken from La Silla Observatory, ESO, by also using narrowband filters (CN, C_2, BC and RC). Nights marked with ⋆ were photometric.

Table 2. Rosetta comet filter extinction coefficients from observations on four photometric nights.

Date UT	BC (mag/AM)	RC (mag/AM)	C_2 (mag/AM)	NH_2 (mag/AM)
Dec. 05 2004	0.165 ± 0.008	0.054 ± 0.003	0.080 ± 0.001	–
Dec. 15 2004	0.220 ± 0.009	0.040 ± 0.001	0.118 ± 0.001	–
Jan. 06 2005	0.180 ± 0.010	0.088 ± 0.004	0.141 ± 0.006	0.109 ± 0.008
Jan. 24 2005	0.285 ± 0.011	0.074 ± 0.008	0.100 ± 0.007	0.094 ± 0.008

Note: BC and RC mean "blue" continuum and "red" continuum filters, respectively, and C_2 and NH_2 mean filters centered on the C_2 and NH_2 emissions. In December 2004 no observations with the NH_2 filter were performed.

Table 3. $Af\rho$ parameter determined from observations on four photometric nights.

Date(UT)	BC $Af\rho_{445}$ (cm)	RC $Af\rho_{687}$ (cm)	Dust color (% per 1000 Å)
Dec. 05 2004	2683 ± 224	3198 ± 66	7.2 ± 3.5
Dec. 15 2004	3139 ± 275	3187 ± 32	0.6 ± 3.6
Jan. 06 2005	4032 ± 113	4216 ± 53	1.8 ± 1.6
Jan. 24 2005	3128 ± 125	3892 ± 53	9.0 ± 1.7

Note: The last column shows the color of the dust coma derived from the $Af\rho$ values at the two different wavelengths.

cometary coma filled the entire field-of-view of the instruments. The extinction coefficients for the observations at Lulin observatory were determined for all nights with photometric sky conditions, using at least three stars observed at a number of different airmasses during the night. The derived extinction coefficients of narrow-band filters are listed in Table 2. These coefficients were used for the extinction correction. Photometric standard stars, GD71 or BD+28 4211, selected from the list presented by Bonev et al. (2003) were observed on photometric nights and used to convert the measured counting rates into physical units. The continuum contribution in the gas-filter images was removed by subtraction of the appropriately scaled continuum determined from the dust filter images. The continuum scaling factor (k) can be calculated by taking into account both the wavelength dependence of the solar spectrum and the effect of the reddened cometary continuum, as discussed later.

Note that in December 2004, no NH_2 images were obtained at Lulin because the filter centered on the NH_2 emission was replaced by a comet ion filter (i.e. CO^+) for observing comet Machholz's ion tail. The observations of comet Machholz's ion tail will be described in a subsequent publication.

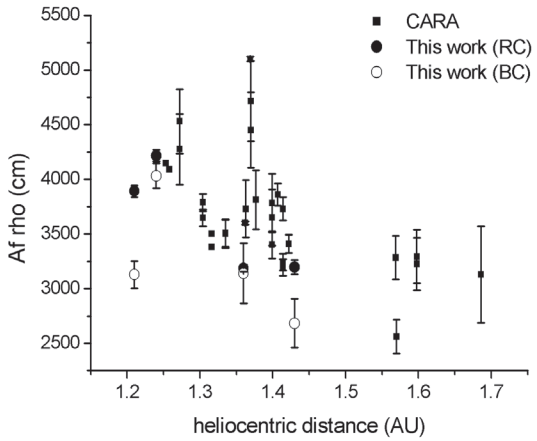

Fig. 1. The variation in $Af\rho$ (only the pre-perihelion points are plotted) with heliocentric distance. The square symbols are given by Sostero & Ligustri (2004, 2005) in the Cometary Archive for Amateur Astronomers (CARA), respectively. The filled and open circles are determined from observations with RC and BC filters in this work.

3. Dust properties and gas production rates

To characterize the dust activity of a comet it has become customary to determine the product of albedo (A), filling factor (f), and the projected radius (ρ) of the aperture in the plane of the comet used for observations, $Af\rho$ (A'Hearn et al. 1984), given by:

$$Af\rho = \frac{(2r\Delta)^2}{\rho} \frac{F_{\rm com}}{F_{\rm sun}}. \quad (1)$$

Here r [AU] is the comet's heliocentric distance, Δ[cm] the comet's geocentric distance, ρ [cm] the radius of aperture at the comet (20 000 km in this work), $F_{\rm com}$[erg cm^{-2} s^{-1}]

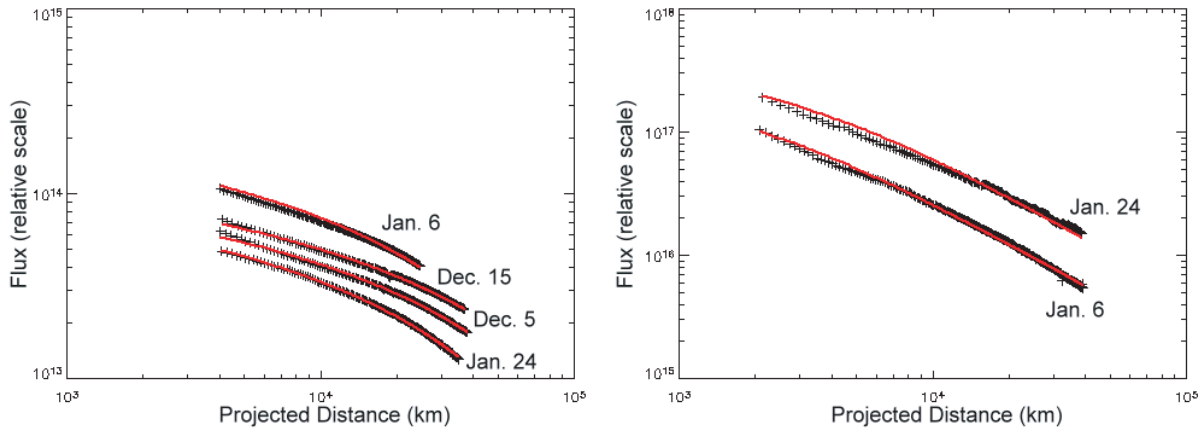

Fig. 2. Mean-radial column-density profiles of C_2 (*left panel*) and NH_2 (*right panel*). The best-fitting Haser profiles are shown by solid curves.

Table 4. Production rates of C_2 and NH_2 and scale lengths, l_p and l_d, of parent and daughter molecules, respectively.

Date(UT)	$Q(C_2)$ 10^{26} molecule s^{-1}	$l_p(C_2)$ 10^4 km	$l_d(C_2)$ 10^5 km	$Q(NH_2)$ 10^{26} molecule s^{-1}	$l_p(NH_2)$ 10^3 km	$l_d(NH_2)$ 10^5 km
Dec. 05 2004	1.07 ± 0.19	2.81 ± 0.35	6.71 ± 0.05			
Dec. 15 2004	1.13 ± 0.26	4.50 ± 0.22	2.52 ± 0.70			
Jan. 06 2005	1.38 ± 0.19	1.88 ± 0.93	3.84 ± 0.84	0.87 ± 0.12	2.12 ± 0.41	5.61 ± 0.29
Jan. 24 2005	3.76 ± 0.63	3.03 ± 0.42	1.25 ± 0.35	1.03 ± 0.17	3.30 ± 0.03	5.30 ± 1.50

the measured cometary flux in a continuum filter, and F_{sun}[erg $cm^{-2}s^{-1}$] the solar flux at 1 AU. The solar flux was computed by using a high-resolution solar spectrum (Kurucz et al. 1984) for determining the solar flux within the wavelength range on which the transmission curve of the comet continuum filters is larger than zero. The $Af\rho$ is related to a stationary model that assumes a uniform and constant dust expansion within the coma. According to this model, the dust column density varies as ρ^{-1}. In this case, $Af\rho$ becomes independent of ρ. The derived values for $Af\rho$ on the four photometric nights are presented in Table 3. In Fig. 1, the $Af\rho$ values are plotted versus heliocentric distance, together with $Af\rho$ values taken from other publications.

3.1. Dust colors

The derived $Af\rho$ values in two filter bandpasses allow for the determination of the color of the cometary dust. The dust color is defined as the gradient of the $Af\rho$ product between the blue (λ_0 = 445 nm) and red (λ_0 = 687.4 nm) continuum points (Jewitt & Meech 1986). The color can be quantified in percentage reddening per 1000 Å, using the relation (Bonev 2002):

$$color = \frac{Af\rho_{687} - Af\rho_{445}}{\lambda_1 - \lambda_2} \frac{2000}{Af\rho_{687} + Af\rho_{445}}, \quad (2)$$

where $Af\rho_{687}$ and $Af\rho_{445}$ are the $Af\rho$ values at wavelength 687.4 nm (λ_1) and 445 nm (λ_2), respectively. The resulting dust colors are presented in Table 3. The average dust color is 4.7% per 1000 Å, which means that the dust coma of comet Machholz is redder than the solar spectrum.

3.2. Gas production rates

In order to determine the gas production rates, the continuum contribution in the gas filter images can be removed by the continuum scaling factor (Kursun et al. 2002). The scaling factor k is given by

$$k = \frac{F^{\odot}_{m+d}}{F^{\odot}_{d}} \left[1 + \frac{Af\rho_{687} - Af\rho_{445}}{\lambda_{687} - \lambda_{445}} \frac{\lambda_{m+d} - \lambda_d}{(Af\rho)_d} \right]. \quad (3)$$

Here the subscripts 687 and 445 refer to the red continuum and blue continuum filters and the subscripts m+d and d refer to gas emission filter and the dust continuum filter nearby (i.e. blue continuum for C_2 and red continuum for NH_2). $F^{\odot}$ denotes the solar flux convoluted with the transmission curve of the filter indicated in the subscript, λ the wavelength.

After the continuum subtraction, the mean radial emission profiles of C_2 and NH_2 were derived from the images obtained in the corresponding filters. We fitted the mean radial brightness profiles of C_2 and NH_2 using the Haser model (Haser et al. 1957), which describes the isotropic emission of cometary

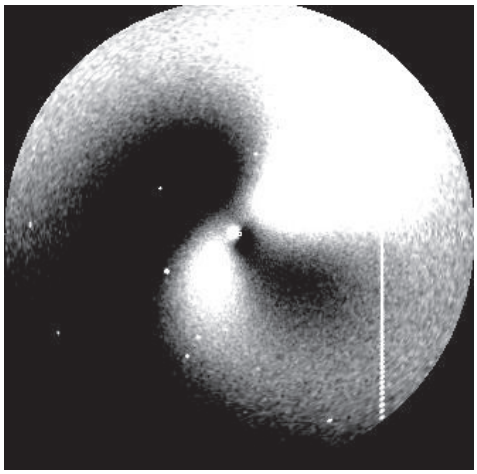

Fig. 3. An image of comet Mochholz taken with CN filter on 2004 Dec. 9 at La Silla Observatory, ESO. The image shows the deviation from the mean coma intensity profile and the gray-stone scale is set between 0.95 and 1.05; North is up, East to the left.

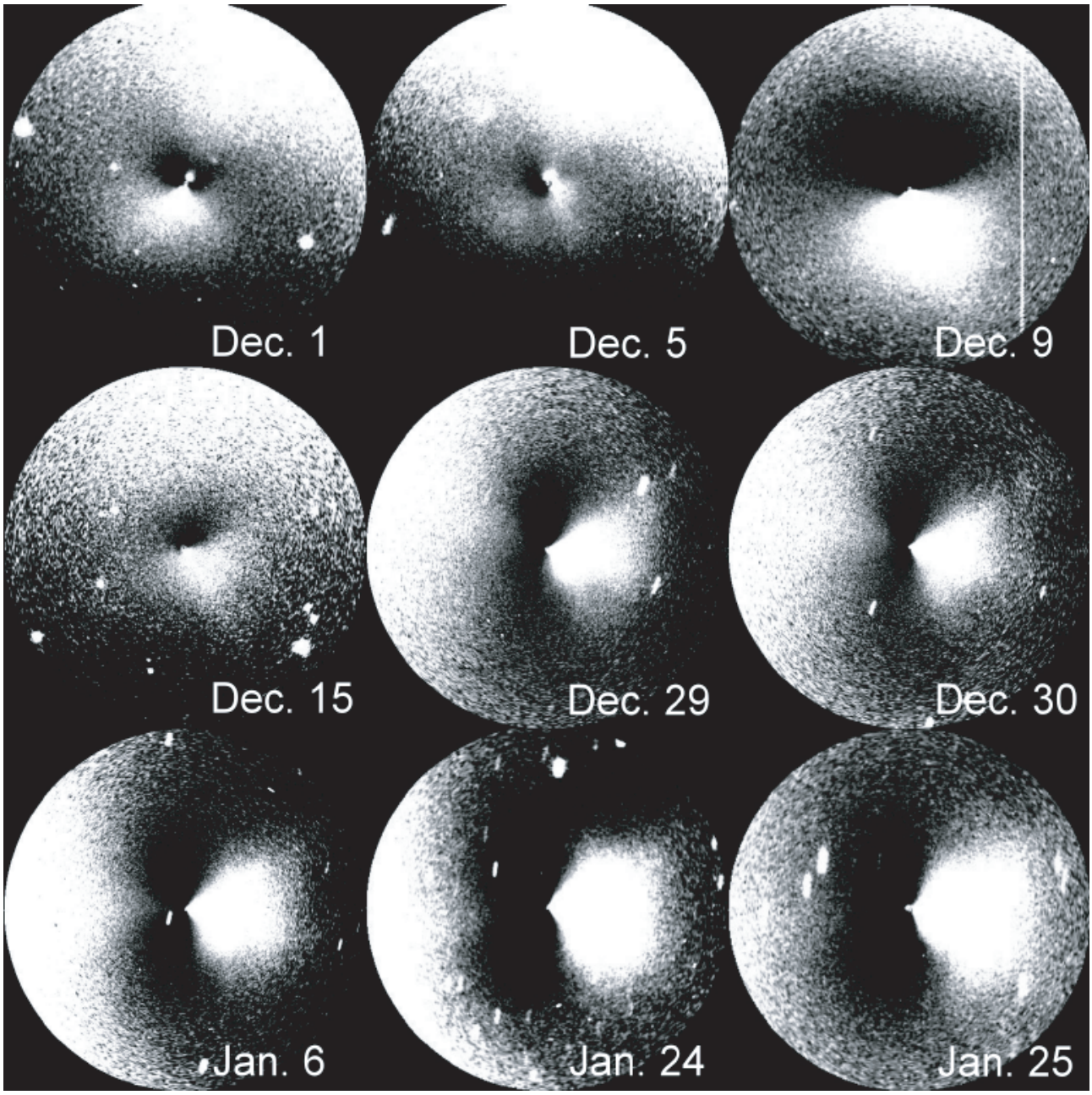

Fig. 4. Sequence of Red continuum images after coma structure enhancement. The nucleus position is at the center of each frame, and the diameter of field of view is 80 000 km. The brightness is scaled ±5% around the mean instensity value. North is up, East to the left, and the arrows indicate the projected solar direction.

neutral molecules and their daughter molecules and radicals. The scale lengths of the parent molecules (l_p) and the daughter molecules (l_d) can be estimated from a fit of the model output to the observational data. These quantities determine the shape of the radial brightness profiles. The derived scale lengths are presented in Table 4. When the brightness profiles are converted into column density profiles, we can then go on to compute the corresponding Haser parent production rates (Q). For the conversion into column density profiles, the fluorescence efficiency factors (g-factors) of C_2 (4.5×10^{-13} erg (molecule s)$^{-1}$), A'Hearn et al. 1995) and NH_2 (2.29×10^{-15} erg (molecule s)$^{-1}$, Korsun et al. 2002) were applied. In this calculations, we assumed that the g-factors varied with the heliocentric distance r (AU) as $g = g_0/r^2$. The mean radial column density profiles derived from the observations during the four photometric nights are plotted in Fig. 2, together with the best-fitting profiles obtained with the Haser model. The production rates of the C_2 and NH_2 Haser parents are summarized in Table 4.

4. Coma morphology and jet activity

To study the morphology of the gas and dust coma of comet Machholz, an image enhancement technique was applied to the present set of images. The mean radial brightness profile of the cometary coma, averaged over all azimuthal angles, was determined in the first step. Then, the comet image was divided by the mean brightness profile to enhance deviations from the mean coma. This method was applied to all images taken in continuum filters, the CN filter, and the C_2 filter (before continuum subtraction). Since the signal-to-noise ratio of the images taken

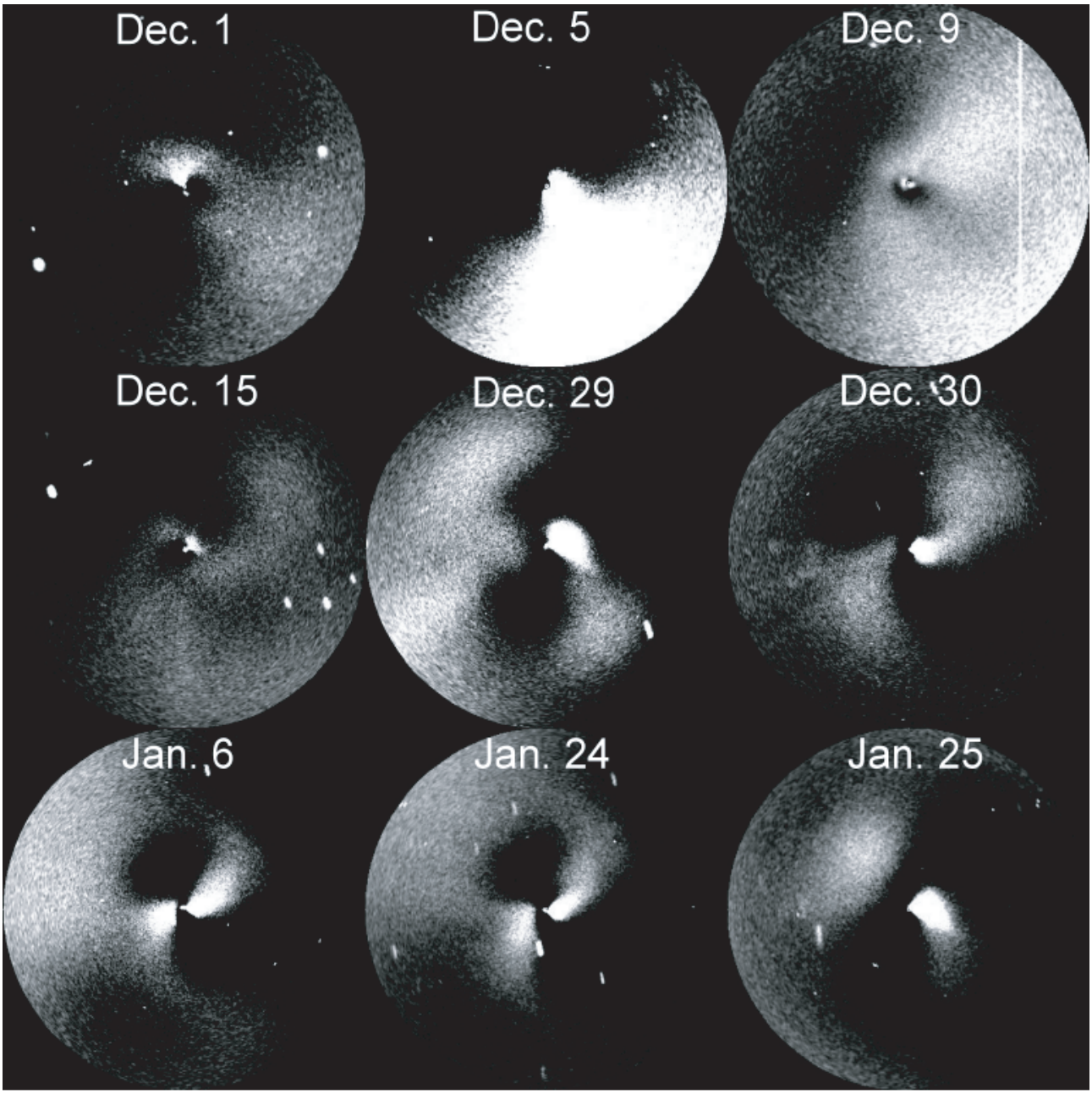

Fig. 5. As in Fig. 4, but for C_2 filter images.

in the NH_2 filters was low, these images are not suitable for an analysis of the coma morphology. The processed C_2 images of the coma of comet Machholz are presented in Fig. 5. The processed C_2 filter images from observations between December 9 and January 24 revealed two jets in the coma of comet Machholz. These jets appeared to be twisted into a spiral-like structure, and the position angles at which the jets are observed clearly changed between December 9 and December 30. Between January 6 and January 24, no change in the position of the two jets was detectable. Between January 24 and January 25, the appearance of the C_2 coma had changed. One jet has disconnected from the nucleus position and an isolated cloud remained in the coma, while the curvature of the second jet has changed. In Fig. 3, two twisted jets could also be revealed in the images taken in the CN filter on December 9. (In all images presented here, North is at the top and East is at the left.)

The processed images taken in the Red continuum filter are shown in Fig. 4. Here, the coma has a different appearance compared to the C_2 images (Fig. 5). The two jets observed in the gas images cannot be detected in the continuum images. The dust coma shows an asymmetry with enhanced brightness in the projected solar direction.

5. Discussion

The observed jets in the gas coma can be explained by the presence of two active regions on the nucleus surface of comet Machholz. The rotation of the nucleus may cause the spiral shape of the jets and its change in position angle with time. Unfortunately, the time coverage of the images is insufficient for deriving the rotation period of the nucleus or the orienting of its rotation axis. The disconnection of one C_2 jet observed between

January 24 and January 25 can be explained if it is assumed that one active surface area has moved out of the sunlight and into the shadow of the nucleus. In such a case, the sublimation of ices from the surface area stops and the area can become inactive within a short time.

The enhancement in brightness in the dust coma is always directed towards the projected solar direction and not correlated to the position of the gas jets. Therefore, it is likely that dust jets and gas jets came from different sources. Organic "CHON" grains (Wickramasinghe & Allen 1986; Kissel et al. 1986a,b) coming from active regions might be a source of CN and C_2 radicals in the jets. These grains are probably not larger than 0.1 μm, so that they were not seen in the reflected continuum, which was dominated by much larger grains (Sekanina 1986). That also explains why the jets observed in the C_2 filter images are weaker than in the CN filter images. The continuum provides a relatively larger contribution to the C_2 filter images than to the CN filter images and itself did not show jet structures.

6. Summary

The summary of our observations of the comet Machholz were showed in the following:

1. For comet Machholz, the average values of the C_2 parent and daughter scale lengths are 3.45×10^4 km and 3.49×10^5 km, respectively. The corresponding values for NH_2 are 2.17×10^3 km and 3.01×10^5 km, respectively. In comparison, the presented values of the C_2 parent and daughter scale lengths are close to our previous measurements (1.8×10^4 km and 2.0×10^5 km) of comet C/2001 A2 (LINEAR) (Lin et al. 2007). The NH_2 parent and daughter scale lengths are comparable to the corresponding value for comet C/1999 J3(LINEAR) (5.0×10^3 km and 1.0×10^5 km) measured by Kousun et al. (2002)
2. The average C_2 and NH_2 Haser parent production rates determined in four nights at heliocentric distances between 1.43 AU and 1.21 AU are $Q(C_2) \sim 1.84 \times 10^{26}$ molecules s^{-1} and $Q(NH_2) \sim 0.95 \times 10^{26}$ molecules s^{-1}, respectively. These values are nearly the same as comet C/2001 A2 (LINEAR) ($Q(C_2) \sim 1.3 \times 10^{26}$ molecules s^{-1} and $Q(NH_2) \sim 0.88 \times 10^{26}$ molecules s^{-1}) but less than two orders of magnitude in comparison to those of comet Hale-Bopp (Rauer et al. 2003).
3. The average $Af\rho$ parameters at wavelengths of λ_0 = 445 nm and λ_0 = 687.4 nm are 3245 cm and 3623 cm on the same interval as heliocentric distances, respectively.
4. The average of dust color is 4.7% per 1000 Å on the wavelength interval [445 nm, 687.4 nm].
5. A morphological analysis of gas coma revealed spiral jets in the CN and C_2 images. These jets are not present in the continuum images. The observed coma structures can be explained by the presence of two active surface regions on a rotating nucleus. However, the dataset is not sufficient to derive the period of the comets rotation. The disconnection of one jet from the nucleus position on January 25 is suggestive of the moving of one active surface region away from the sunlit direction.

Acknowledgements. This work was based on observations obtained at Lulin Observatory whose staff and the assistants kindly help me to finish these observations. The research carried out was supported by NSC95-2111-M-008-006.

References

A'Hearn, M. F., Schleicher, D. G., Feldmann, P. D., Millis, R. L., & Thompson, D. T. 1984, AJ, 89 579
A'Hearn, M. F., Hoban, S., Birch, P. V., et al. 1986, Nature, 327, 649
A'Hearn, M. F., Millis, R., Schleicher, D. G., Osip, D. J., & Birch, P. V. 1995, Icarus, 118, 223
Bockelee-Morva, D., Crovisier, J., Mumma, M. J., & Weaver, H. A. 2004, in Comet II, ed. M. C. Festou, H. U. Keller, & H. A. Weaver (Tucson: University of Arizona Press), 745, 449
Bonev, T., Jockers, K., Petrova, E., et al. 2002, Icarus, 160, 419
Haser, L. 1957, Bull. Acad. R. Sci. Leige, 43, 740
Jewitt, D., & Meech, K. J. 1986, ApJ, 310, 937
Kawakita, H., Watanabe, J., & Kinoshita, D. 2001, ApJ, 572, L177
Kinoshita, D., Huang, K. Y., Wu, Y. L., Chang, Y. H., & Urata, Y. 2003, Lulin Observatory Report, 30
Kinoshita, D., Chen, C. W., Lin, H. C., et al. 2005, CHJAA, 5, L315
Kissel, J., Brownlee, D. E., Buchler, K., et al. 1986a, Nature, 321, 280
Kissel, J., Sagdeev, R. Z., Bertaux, J. L., et al. 1986b, Nature, 321, 336
Kurucz, R. L., Furenlid, I., Brault, J., & Testerman, L. 1984, Solar flux atlas from 296 to 1300 nm (Sunspot, New Mexico: National Solar Observatory)
Korsun, P. P., & Jockers, K. 2002, A&A, 381, L703
Lara, L.-M., Tozzi, G. P., Boehnhardt, H., DiMartino, M., & Schulz, R. 2004, A&A, 422, 717
Lin, Z. Y., Chang, C. P., & Ip, W. H. 2007, AJ, 133, L1861
Rauer, H., Helbert, J., Arpigny, C., et al. 2003, A&A, 397, 1109
Sastri, J. H., Vasundhara, R., Kuppuswamy, K., & Velu, C. 2005, IAUC., 8480
Sekanina, Z. 1986, Adv. Space Res., 5, 307
Wickramasinghe, D. T., & Aleen, D. A. 1986, Nature, 323, 44